Chemical Science

Dynamic Article Links

Cite this: *Chem. Sci.*, 2012, **3**, 384

www.rsc.org/chemicalscience

EDGE ARTICLE

The luminescence of $Na_xEu^{3+}_{(2-x)/3}MoO_4$ scheelites depends on the number of Eu-clusters occurring in their incommensurately modulated structure†

Alla Arakcheeva,*[a] Dmitry Logvinovich,[ab] Gervais Chapuis,[a] Vladimir Morozov,[c] Svetlana V. Eliseeva,[d] Jean-Claude G. Bünzli[de] and Philip Pattison[af]

Received 13th May 2011, Accepted 10th August 2011
DOI: 10.1039/c1sc00289a

Scheelite related compounds with general formula $M_n(XO_4)_m$ are the subject of hefty interest owing to their optical properties, stability and relatively simple preparation. Eu^{3+}-containing scheelites are considered as red-emitting phosphors and the main factors affecting their luminescence are thought to be chemical composition and particle size while the influence of their structure is generally ignored. Here we report eight compounds from the $Na_xEu_{(2-x)/3}MoO_4$ series prepared by conventional solid-state reaction and present a detailed analysis of their crystal structures. Six of them have modulated structures, a common feature of SRCs, in which dopant Eu^{3+} ions are orderly distributed. Moreover, different amounts of Eu^{3+} dimers are detected in the modulated structures, characterized by weak satellite reflections appearing in the lower angle part of the XRD patterns. These reflections are indexed and incorporated into Rietveld's refinement using superspace (3 + 1)-dimension symmetry. The remarkable feature of the compounds is that the characteristic luminescence parameters, overall (Q_L^{Eu}) and intrinsic (Q_{Eu}^{Eu}) quantum yields, Eu($^5D_0$) lifetimes, and sensitization efficiencies (η_{sens}), correlate with the number of Eu^{3+} aggregates, but not directly with the composition x of the materials. This provides an efficient tool for understanding and controlling the luminescence properties of scheelite related compounds.

[a]*Laboratoire de cristallographie, École Polytechnique Fédérale de Lausanne, 1015 Lausanne, Switzerland. E-mail: allaarakcheeva@gmail.com*
[b]*ETH Honggerberg Laboratorium für Kristallographie, 8093 Zürich, Switzerland*
[c]*Department of Chemistry, Moscow State University, 119991 Moscow, Russia*
[d]*Institute of Chemical Sciences and Engineering, École Polytechnique Fédérale de Lausanne, 1015 Lausanne, Switzerland*
[e]*WCU Center for Next Generation Photovoltaic Devices, Korea University, Jochiwon, Republic of Korea*
[f]*Swiss-Norwegian Beam Lines at ESRF Grenoble BP-220, 38043, France*

† Electronic supplementary information (ESI) available: Table S1: Chemical, crystallographic data and characteristics of the structure refinements for the $Na_xEu_{(2-x)/3}MoO_4$ compounds. Details of the crystal structure refinements. Diagram S1: Schematic representation of the occupation modulation function of the M position. Fig. S1: Rietveld plots of the $Na_xEu^{3+}_{(2-x)/3}MoO_4$ compounds. Table S2: Final coordinates, isotropic displacement parameters and Fourier amplitudes of the displacive modulation functions for $Na_xEu_{(2-x)/3}MoO_4$. Details of the estimation of the amount of Eu atoms forming isolated Eu-clusters. Fig. S2: Schematic representation of the M cationic subset with statistical distribution of cations in $Na_xEu_{(2-x)/3}MoO_4$. Fig. S3: Schematic presentation of the M cationic subset with a typical ordered distribution of Eu, Na and vacancies in $Na_xEu_{(2-x)/3}MoO_4$ and t-plots of the Eu1–Eu distances. Table S3: Estimation of the amount of Eu atoms forming isolated Eu-clusters on the basis of Eu–Eu distances in $Na_xEu_{(2-x)/3}MoO_4$. Table S4: Details of the luminescence characteristic measurements and the corresponding relative number of the Eu-clusters for the $Na_xEu^{3+}_{(2-x)/3}MoO_4$ compounds. Fig. S4: Relative intensities of the emission spectra as a function of composition of $Na_xEu^{3+}_{(2-x)/3}MoO_4$. CCDC reference numbers 735548 and 825869–825873. For ESI and crystallographic data in CIF or other electronic format see DOI: 10.1039/c1sc00289a

Introduction

Scheelite related compounds (SRCs) (Fig. 1) with general formula $M_n(XO_4)_m = M_{n/m}(XO_4)$ cover a broad spectrum of compositions, with M being either a single element or a combination of up to three cations, which can be alkaline elements, Ca, Sr, Pb, Ba, Zn, Cd, In, Ga, Tl, Ln, Y and Bi, while X is Mo, W, Nb, V, Ta or, possibly, a combination thereof. They are highly stable and their preparation by solid-state reaction is easy so that scheelites are found in many industrial applications, including solid oxide fuel cells[1,2] and photocatalysts.[3] Presently, much attention is also being drawn on some SRCs in view of their interesting optical properties. For instance, Eu^{3+}-containing SRCs are currently being investigated owing to their promising red-emission phosphor capacity for three-band white-light-emitting diodes (WLEDs).[4–10] The chemical composition[11] and size of the particles are important factors affecting the luminescence of SRC phosphors. Influence of the crystal structure on the luminescence properties has been discussed for some SRCs.[12] However, this aspect is usually ignored because only statistical distributions can be derived for different M cations by conventional crystallographic methods. On the other hand, application of the (3 + 1)-dimensional symmetry concept[13] shows that the entire family of compositionally different SRCs can be described from a unique model of modulated structures, which is characterized by a fully ordered distribution of different cations in the M subset.[14] The vast majority of the published SRCs exhibit the stoichiometry $M : XO_4 = m/n = 1$ leaving no possibilities for vacancies in the M subset. Only charge neutrality limits the m/n ratio in the modulated

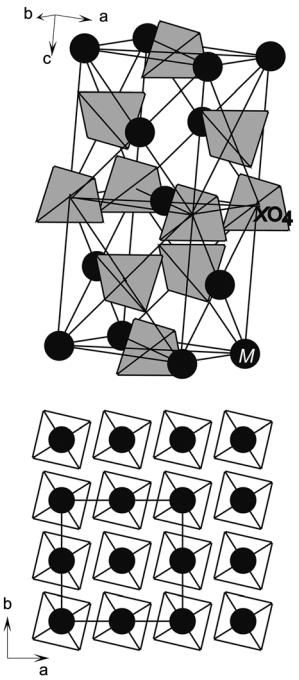

Fig. 1 The typical scheelite-like structure and its *ab* projection.

structure model. Hence, this model allows one to predict SRCs with completely ordered structures within a wide and continuous range of compositions. The modulated structures can be identified by the presence of additional satellite reflections in the lower angle part of XRD patterns.[14] These weak reflections are usually ignored. However, they provide an invaluable source of information on the atomic ordering which can be extracted by application of the (3 + 1)-dimension symmetry model. As a consequence, correlation between crystal structure and luminescence parameters can be much more precisely deciphered than in previous work.[12]

In this paper, we exemplify the potential of this concept with the $Na_xEu^{3+}{}_{(2-x)/3}MoO_4$ ($0 \leq x \leq 0.5$) series by solving the structure of six samples of different composition and relating their photophysical parameters to the nature and amount of Eu aggregates present in the scheelites.

Experimental

Preparation and chemical composition

$Na_xEu^{3+}{}_{(2-x)/3}\Delta_{(1-2x)/3}MoO_4$ (Δ indicates vacancies in the M subset) molybdenum oxides were synthesized from a stoichiometric mixture of Na_2MoO_4 (99.99%), Eu_2O_3 (99.99%), and MoO_3 (99.99%) by the solid-state method at $T = 1023$ K for 48 h in air followed by quenching from $T = 1023$ K to room temperature. Nine different compositions defined by x spanning the $0 \leq x \leq 0.5$ range have been prepared (Table 1). Element contents were determined by inductively coupled plasma optical emission spectrometry (ICP-OES) and, independently, from the refinement of their crystal structures (Table 1).

X-Ray diffraction experiments

Powder diffraction data were collected on the Swiss-Norwegian Beam Line BM01A at the ESRF, Grenoble. The wavelengths were selected using a Si(111) double crystal monochromator, and the synchrotron beam was focused onto a spot size of 0.3 mm × 0.3 mm using a combination of curved mirrors and a sagittally bent second crystal. All samples were filled into borosilicate capillaries of 0.5 mm diameter, and the data were collected at room temperature. A mar345 image plate detector was used to register the powder patterns. The sample-to-detector distance of 250 mm was calibrated using a LaB_6 reference powder. Exposure times per sample were typically 30 s per image and the samples were rotated during data collection at a speed of $1^\circ\ s^{-1}$. Exposure times were chosen to avoid any pixel saturation. The Rietveld refinement of the $Na_xEu^{3+}{}_{(2-x)/3}MoO_4$ structures has been performed using the *JANA2006* program package.[15] The anisotropic microstrain line-broadening[16] has been applied for the profile descriptions. $Na_{0.5}Eu_{0.5}MoO_4$ and $Na_{0.286}Eu_{0.571}MoO_4$ have been refined in the conventional $I2_1/a$ space group with statistically distributed cations Na and Eu. According to the scheme proposed for SRC,[14] the $I2/b(\alpha\beta0)00$ (3 + 1)D superspace group has been applied here for all other incommensurately modulated structures and earlier for $Eu^{3+}{}_{2/3}MoO_4$.[17] The phase with $x = 0.134$ has been refined along with 6% of an additional phase with $x = 0.015$. The crystallographic data are shown in Table 1. The experimental XRD patterns and their magnified lower angle parts of the $Na_xEu^{3+}{}_{(2-x)/3}MoO_4$ compounds are shown in Fig. 2 and 3 respectively. All details of the Rietveld refinements, the experimental, calculated and difference diffraction profiles are available in ESI† ("Details of the crystal structure refinements", Table S1, Diagram S1, and Fig. S1). The Rietveld plot of calculated and difference profiles obtained for the two-component samples are shown in Fig. 4 as an example. The details of the crystal structures (Table S2, ESI†) may be obtained from the Fachinformationszentrum Karlsruhe, 76344 Eggenstein-Leopoldshafen (Germany), on quoting the depository numbers CSD-420696 ($Na_{0.5}Eu_{0.5}MoO_4$), CSD-420697 ($Na_{0.25}Eu_{0.583}MoO_4$), CSD-420698 ($Na_{0.236}Eu_{0.588}MoO_4$), CSD-420699 ($Na_{0.2}Eu_{0.6}MoO_4$), CSD-420700 ($Na_{0.138}Eu_{0.621}MoO_4$), CSD-420701 ($Na_{0.134}Eu_{0.622}MoO_4$).

Luminescence study

Emission and excitation spectra as well as quantum yields were measured at room temperature with a Fluorolog FL3-22 spectrofluorimeter from Horiba-Jobin-Yvon Ltd on well-ground powder samples placed in quartz capillaries with an internal diameter of 2.4 mm. Quantum yields were determined at room temperature under excitation of MoO_4^{2-} anion at $\lambda = 320$ nm (Q_L^{Eu}) and of the Eu($^5D_2$) level at $\lambda = 465$ nm (Q_{Eu}^{Eu}) using an absolute method based on a specially modified integration sphere with 2-inch diameter[18] from GigaHertz Optik® in Zenith® Teflon. Each sample was measured several times under slightly different experimental conditions. The estimated error for quantum yields is 10%. All the excitation and luminescence spectra were corrected for instrumental functions. Lifetime measurements were performed at room temperature and at 77 K on the same samples using a Quantum Brillant Nd:YAG laser equipped with frequency tripler ($\lambda_{exc} = 355$ nm). Luminescence decays were measured upon monitoring the $^5D_0 \rightarrow {}^7F_2$ transition and analyzed with Origin® 7.0; all of them proved to be single exponential functions at 77 K but bi-exponential functions were

Table 1 Chemical and crystallographic characteristics of $Na_xEu_{(2-x)/3}MoO_4$ compounds

Refined composition (found by ICP-OES)	Lattice constants (Å, °)	Modulation vector $\boldsymbol{q} = \alpha\boldsymbol{a}^* + \beta\boldsymbol{b}^*$
$Na_{0.5}Eu_{0.5}MoO_4$[a] ($Na_{0.54(2)}Eu_{0.505(5)}Mo_{1.00(1)}$)	$a = 5.2421(1)$ $b = 5.2385(1)$ $c = 11.4543(2)$ $\gamma = 89.949(3)$	None
$Na_{0.286}Eu_{0.571}MoO_4$[a] ($Na_{0.285(5)}Eu_{0.572(6)}Mo_{1.000(15)}$)	$a = 5.2391(1)$ $b = 5.2393(1)$ $c = 11.4954(2)$ $\gamma = 90.049(3)$	None
$Na_{0.25}Eu_{0.583}MoO_4$[b] ($Na_{0.248(5)}Eu_{0.584(6)}Mo_{1.000(2)}$)	$a = 5.2393(2)$ $b = 5.2395(2)$ $c = 11.5155(1)$ $\gamma = 90.058(2)$	$0.5752(2)\boldsymbol{a}^* - 1.1939(2)\boldsymbol{b}^*$
$Na_{0.236}Eu_{0.588}MoO_4$[b] ($Na_{0.240(8)}Eu_{0.587(6)}Mo_{1.00(1)}$)	$a = 5.2395(1)$ $b = 5.2382(1)$ $c = 11.5089(2)$ $\gamma = 90.042(1)$	$0.5721(1)\boldsymbol{a}^* - 1.1917(1)\boldsymbol{b}^*$
$Na_{0.2}Eu_{0.6}MoO_4$[b] ($Na_{0.214(4)}Eu_{0.602(6)}Mo_{1.000(14)}$)	$a = 5.2329(3)$ $b = 5.2339(3)$ $c = 11.5210(2)$ $\gamma = 89.939(3)$	$0.5754(2)\boldsymbol{a}^* - 1.1945(2)\boldsymbol{b}^*$
$Na_{0.138}Eu_{0.621}MoO_4$[b] ($Na_{0.142(4)}Eu_{0.619(5)}Mo_{1.00(1)}$)	$a = 5.2388(1)$ $b = 5.2442(1)$ $c = 11.5592(2)$ $\gamma = 90.1776(5)$	$0.5860(5)\boldsymbol{a}^* - 1.2033(1)\boldsymbol{b}^*$
$Na_{0.134}Eu_{0.622}MoO_4$[b,c]	$a = 5.2318(3)$ $b = 5.2310(3)$ $c = 11.5331(2)$ $\gamma = 90.232(2)$	$0.5987(2)\boldsymbol{a}^* - 1.2134(2)\boldsymbol{b}^*$
$Na_{0.015}Eu_{0.662}MoO_4$[b,c]	$a = 5.228(3)$ $b = 5.230(3)$ $c = 11.486(4)$ $\gamma = 90.98(4)$	$0.6613(8)\boldsymbol{a}^* - 1.3265(1)\boldsymbol{b}^*$
$Eu_{2/3}MoO_4$[d]	$a = 5.2328(3)$ $b = 5.2214(3)$ $c = 11.4529(6)$ $\gamma = 92.414(2)$	$2/3\boldsymbol{a}^* - 4/3\boldsymbol{b}^*$

[a] $I2_1/a$ 3D space group.[b] $I2/b(\alpha\beta0)00$ (3 + 1)D superspace group.[c] $Na_{0.091(2)}Eu_{0.636(7)}Mo_{1.000(11)}$ found by ICP-OES for the sample containing 94% $Na_{0.134}Eu_{0.622}MoO_4$ + 6% $Na_{0.014}Eu_{0.662}MoO_4$.[d] Data after ref. 17.

found at room temperature with a faster decaying component accounting for 6–14%, except for $x = 0$ and 0.286. Reported lifetime data are averages of at least three independent measurements.

Theoretical basis of the luminescence data interpretation

The overall quantum yield Q_L^{Eu} obtained upon excitation in the electronic levels of the molybdate ions is the product of two parameters, the efficiency η_{sens} with which the molybdate ions transfer energy on the Eu^{3+} excited states and the intrinsic quantum yield Q_{Eu}^{Eu} determined by direct excitation into a f-level:[19]

$$Q_L^{Eu} = \eta_{sens} Q_{Eu}^{Eu} \quad (1)$$

Q_{Eu}^{Eu} can be measured provided that the absorption of the excitation f–f transition is large enough to be determined accurately. Tests at $\lambda_{exc} = 465$ nm confirmed the possibility of obtaining Q_{Eu}^{Eu} data by direct measurements. However, the broad absorption band of MoO_4^{2-}, which could overlap with the f–f absorption, can affect these measurements. In principle, Q_{Eu}^{Eu} can alternatively be calculated from the observed (τ_{obs}) and radiative (τ_{rad}) lifetimes by the formulae:

$$Q_{Eu}^{Eu} = \tau_{obs}/\tau_{rad} \quad (2)$$

$$1/\tau_{rad} = A_{MD,0} n^3 (I_{tot}/I_{MD}) \quad (3)$$

where $A_{MD,0} = 14.65\ s^{-1}$ is the spontaneous emission probability for the magnetic dipole $^5D_0 \rightarrow {}^7F_1$ transition in vacuum, n is the refractive index of the material and I_{tot}/I_{MD} is the ratio of the

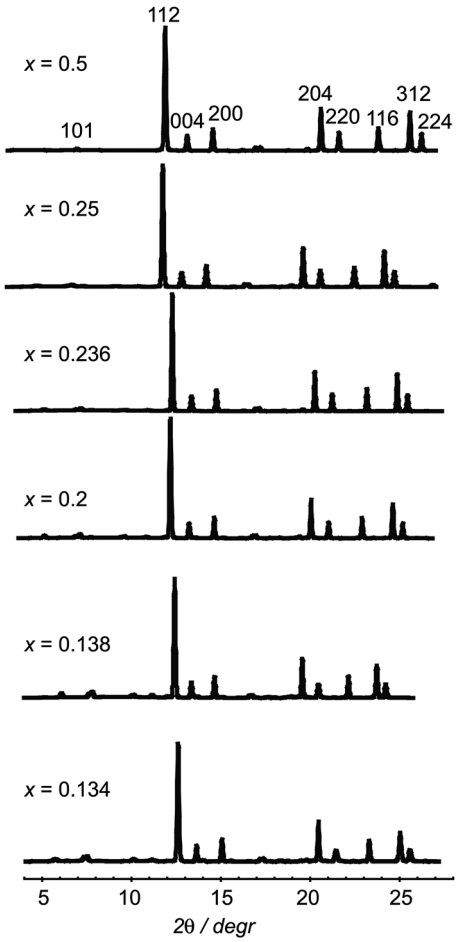

Fig. 2 Experimental XRD patterns of the $Na_xEu^{3+}{}_{(2-x)/3}MoO_4$ compounds with different compositions defined by x. Indices of the strongest reflections are given for the typical scheelite unit cell. The lower angle parts of the patterns are shown separately in Fig. 3.

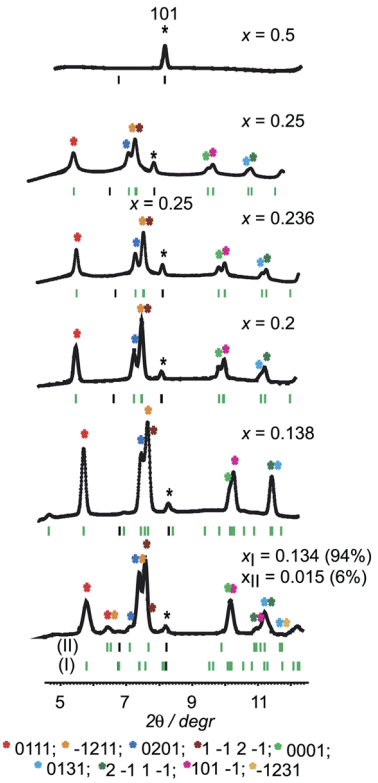

Fig. 3 Magnified lower angle parts of the experimental XRD patterns of $Na_xEu^{3+}{}_{(2-x)/3}MoO_4$ compounds with different compositions defined by x. Colored stars (corresponding to the nine different *hklm* indexes) and green strips indicate the satellite reflections.

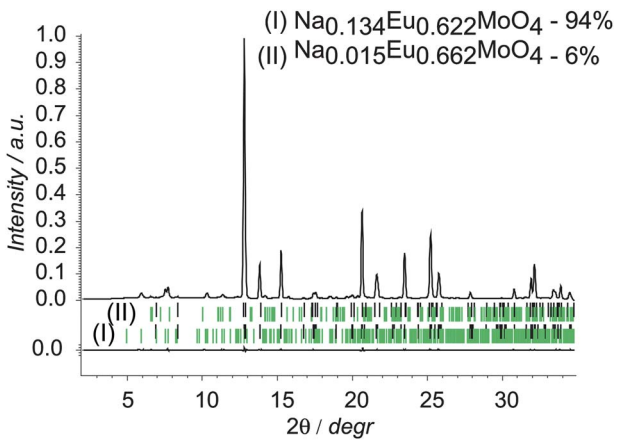

Fig. 4 Rietveld plots of calculated and difference profiles of the sample consisting of 94% phase with $x = 0.134$ and 6% phase with $x = 0.015$. The black and green strips indicate the positions of main and satellite reflections, respectively.

total integrated intensity of Eu^{3+} emission to the integrated $^5D_0 \rightarrow {}^7F_1$ transition. In our case, however, the refractive indices are not known, so that we have proceeded differently, using the equations to determine n values: first, τ_{rad} data were calculated from the Q_{Eu}^{Eu} and τ_{obs} experimental values for each composition which, in turn, allowed estimating refractive indices from eqn (3). Finally, the mean index value was implemented in eqn (3) and Q_{Eu}^{Eu} were estimated from eqn (2) and compared with the experimental data for consistency.

Results and discussion

Specific features of crystal structures

The crystal structures belong to the well-known scheelite type affected by a small monoclinic distortion.[14] The lattice constants of the studied SRCs are very similar (Table 1). The positions of the MoO_4 tetrahedra are alike in the compounds and similar to all other monoclinic scheelites. The XRD patterns are typical for SRCs and they are very analogous for all $Na_xEu^{3+}{}_{(2-x)/3}MoO_4$ compounds (Fig. 2).

The main differences can be observed in the low-angle part of the XRD patterns where satellite reflections can be clearly identified for five samples ($x = 0.25$, 0.236, 0.20, 0.138 and 0.134; Fig. 3). These satellites point to incommensurately modulated structures, while $Na_{0.5}Eu_{0.5}MoO_4$ and $Na_{0.286}Eu_{0.571}MoO_4$ do not display satellites and therefore lack modulation. The structures differ by the distributions of the Na and Eu cations and vacancies on the cationic subset characterized by the two-fold symmetry axis. These distributions are illustrated in Fig. 5 as portions of the *ab* projections of the cationic subset, which is

ordered but aperiodic in a and b directions for the modulated structures. The cations are statistically distributed in the two non-modulated compounds. The specific coefficients α and β of the modulation vector $\boldsymbol{q} = \alpha\boldsymbol{a}^* + \beta\boldsymbol{b}^*$ (Table 1) and individual parameters of three atomic domains, Eu1, Eu2 and Na, constituting one cationic position (Table S2, ESI†), define specific ordering of the cations for each modulated structure. Two types of Eu-aggregates can be distinguished in the ordered structures: first, the Eu^{3+}-dimers or diatomic clusters (Fig. 5) similar to those evidenced recently in silicate AV-24, $K_7[Ln_3Si_{12}O_{32}]\cdot xH_2O$.[20] Secondly, complex layers which are parallel to the c axis and normal to the modulation vector $\boldsymbol{q}$.

The shortest Eu–Eu distance is equal to about 3.95 Å in both types of Eu-aggregates, whereas the shortest Eu–Eu distance between aggregates is longer than 5.1 Å. In the ab projection of a portion of cationic subsets (Fig. 5), the Eu^{3+}-dimers can be recognized as Eu-pairs isolated from all other Eu-atoms by Na^+ cations and vacancies.

Specific features of the Eu-centered luminescence

Excitation spectra of $Na_xEu^{3+}{}_{(2-x)/3}MoO_4$ (Fig. 6, *a*) present two features: a broad band in the range 250–355 nm with maximum at ≈275 nm due to MoO_4^{2-} anions and several sharp bands in the range 355–570 nm attributable to f–f transitions.

The relative intensity of the former band to the latter ones decreases with decreasing Na content from $x = 0.5$ to 0. Emission spectra (Fig. 6b) recorded under excitation in the molybdate levels display only the characteristic sharp emission lines from the Eu($^5D_0$) level. Ligand-field splitting and relative integral intensities of $^5D_0 \rightarrow {}^7F_J$ transitions ($J = 0$–4) exhibit only slight variations with composition. All luminescence spectra are dominated by the $^5D_0 \rightarrow {}^7F_2$ transition, which represents 75–80% of the total emission, an interesting feature for phosphor applications.

Characteristic parameters of the Eu-centered luminescence have been determined experimentally, namely overall quantum yields, Q_L^{Eu}, observed lifetimes, τ_{obs}, intrinsic quantum yields, Q_{Eu}^{Eu}, from which the efficiency of the MoO_4^{2-}-to-Eu^{3+} energy transfer, η_{sens}, could be calculated. These parameters are presented on Fig. 7 as a function of the $Na_xEu^{3+}{}_{(2-x)/3}MoO_4$ compositions. The overall quantum yield and observed lifetimes both exhibit a non-monotonic variation as a function of composition. The maximal values of Q_L^{Eu} and τ_{obs} correspond to disordered $Na_{0.5}Eu_{0.5}MoO_4$, which has been reported before as a red-emission phosphor.[21–23] The lowest value of both parameters is observed for $Eu_{2/3}MoO_4$. The overall tendency for these two parameters to increase with increasing Na concentration is interrupted by two minima at $x = 0.286$ and 0.2. On the other hand, the sensitization efficiencies calculated from eqn (1) display a smooth but substantial increase from 4% for $x = 0$ to 38% for $x = 0.5$, pointing to MoO_4^{2-} anions introducing a linear effect in the variation of Q_L^{Eu} with composition. In absence of experimental refractive index data, we have recalculated n values by combining eqn (2) and (3). The obtained mean $n = 1.75(11)$ is a reasonable value for such compounds, for instance $n = 1.82$ has been reported for orthorhombic europium molybdate.[24] The average n value has been used to recalculate intrinsic quantum yields and the recalculated Q_{Eu}^{Eu} values are in good agreement with the measured ones (to within ±20%), given experimental uncertainties, except for the non-modulated sample with $x = 0.5$. This demonstrates that MoO_4^{2-} absorption interferes little with the f–f-transitions at the wavelength used for the determination of the intrinsic quantum yields. The latter display a variation

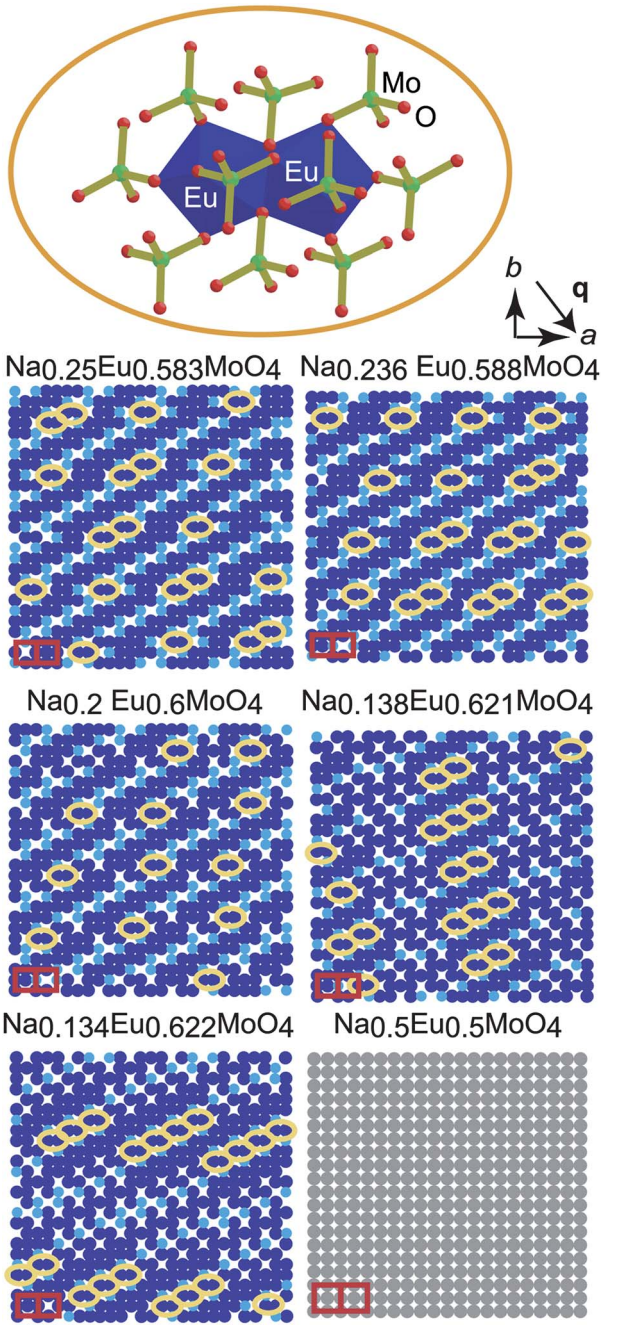

Fig. 5 Portions of the *ab* projection of the cation subset in $Na_xEu^{3+}{}_{(2-x)/3}MoO_4$ compounds. Dark and light blue colors correspond to Eu and Na atoms, respectively, in the aperiodically ordered structures; grey indicates a mixture (Eu, Na) position in the disordered structure. Vacancies appear as large white stars. Eu dimers are surrounded by yellow contours. In the aperiodically ordered structures, the cation distribution differs in each adjacent unit cell (examples are indicated by red squares), whereas they are identical in the disordered one. On the top, the nearest surrounding of a single Eu dimer is shown separately.

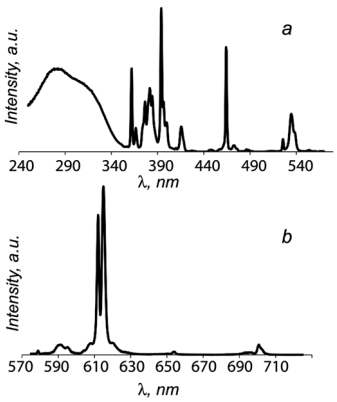

Fig. 6 Excitation (a) and emission (b) spectra of $Na_{0.2}Eu^{3+}{}_{0.6}MoO_4$ as representative examples for the series.

with composition reminiscent of that discussed for the overall quantum yield. Thus we may conclude that differences in the structural characteristics of the Eu-subsets are responsible for the observed non-monotonous behavior of the luminescent parameters, which leads us to the following analysis.

Correlation of luminescence parameters with the number of Eu^{3+} clusters

To substantiate the above conclusion, we have plotted the luminescence parameters *vs*. the relative number of Eu in the clusters, $N_{Eu\text{-}cl}/N_{Eu\text{-}total}$, per unit chemical formula $Na_xEu^{3+}{}_{(2-x)/3}MoO_4$. $N_{Eu\text{-}cl}$ has been directly taken from the t-plot of Eu1–Eu distances for each modulated compound (Fig. S3 and Table S3, ESI†). For $Na_{0.286}Eu_{0.571}MoO_4$ and $Na_{0.5}Eu_{0.5}MoO_4$ with statistical distribution of Na, Eu and vacancies on cationic positions, $N_{Eu\text{-}cl}$ has been estimated as the sum of probabilities of both isolated Eu^{3+} ions (monoatomic clusters) and Eu^{3+} dimers (diatomic clusters, Fig. S2, ESI†). For a compound with ratio Eu/Na = *a*/*b*, the probability is $p_n = n^2(b/(a+b))^{2(n+1)}(a/(a+b))^{n-1}$, where $n = 1$ and 2 correspond to mono- and diatomic clusters, respectively (see Estimation of the amount of Eu atoms forming isolated Eu-clusters, ESI†). Only Eu layers are present in $Eu_{2/3}MoO_4$, however, very common structural defects such as crystallographic shifts along [100] can result in diatomic clusters. Hence, for this compound, we estimated $N_{Eu\text{-}cl} = 0.0025$, which corresponds to 1% of defect unit cells. The corresponding dependences are shown in Fig. 8 and contrary to the data plotted in Fig. 7, the correlations are now reasonably linear, within experimental errors, which fully validates our hypothesis.

A more detailed analysis has been carried out for the Eu($^5D_0$) lifetime data which have been measured at two temperatures, 293 and 77 K. At room temperature, the decays are bi-exponential with a short component (17–59 μs, $B_2 = 6$–14%), except for $x =$

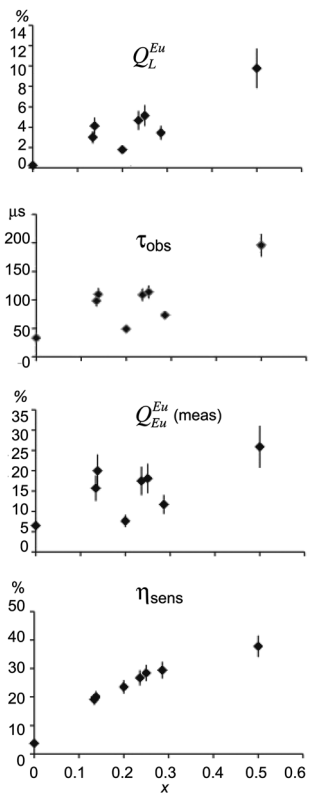

Fig. 7 Overall quantum yields, Q_L^{Eu}, observed lifetimes, τ_{obs}, intrinsic quantum yields, Q_{Eu}^{Eu} (meas), and efficiency of the MoO_4^{2-}-to-Eu^{3+} energy transfer, η_{sens}, as a function of the $Na_xEu^{3+}{}_{(2-x)/3}MoO_4$ composition.

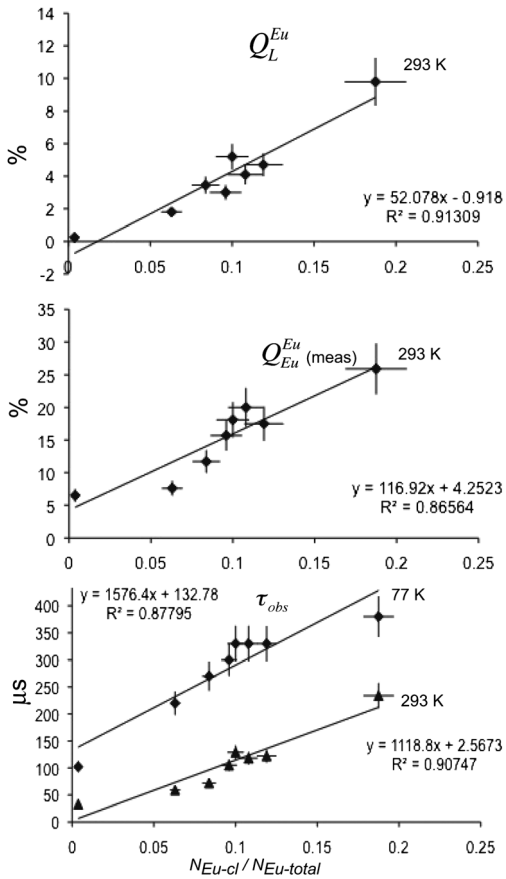

Fig. 8 Quantum yield, Q_L^{Eu}, obtained upon ligand excitation at 293 K, observed lifetimes τ_{obs} at 293 and 77 K, and intrinsic quantum yield of Eu^{3+}, Q_{Eu}^{Eu} (meas), as a functions of the relative amount of Eu^{3+}-clusters, $N_{Eu\text{-}cl}/N_{Eu\text{-}total}$, in $Na_xEu^{3+}{}_{(2-x)/3}MoO_4$.

0.286 and 0, so that average lifetimes have been considered ($<\tau> = \sum_i B_i\tau_i^2 / \sum_i B_i\tau_i$). On the other hand, the decays are single exponential functions at 77 K and the values of τ_{obs} increase about two-fold compared with those at room temperature. This fact points to temperature-dependent nonradiative energy-transfer processes between different sets of Eu^{3+} ions. The single exponential decay observed for $x = 0.286$ and $x = 0$ corresponds to a single crystallographic position statistically occupied by Eu^{3+} and Na^+ ions in their 3D non-modulated structures (Table S4, ESI†). The bi-exponential decay behavior observed at 293 K for all other compounds (Table S4, ESI†) is associated with two atomic domains, Eu1 and Eu2, which are characterized by their (3 + 1)-dimensionally modulated structures (Diagram S1 and Table S2, ESI†). The large contribution of one exponential component at 293 K (86–94%) and the bi-to-single exponential behavior transformation observed for the decays at 77 K seem to be reasonable because only one atomic domain, namely Eu1, constitutes the diatomic clusters (Fig. 7), which mainly contribute to quantum yields. At lower temperature, luminescence intensity from the diatomic Eu1-clusters increases faster,[20] and the lower-percent component, 6–14%, corresponding to Eu2 becomes undetectable. Hence, the behavior of the decays directly correlates with the Eu^{3+} crystallographic characteristics, which are different for 3- and (3 + 1)-dimension structural symmetry.

Conclusions

The luminescence properties of scheelite related compounds are essentially affected by the presence of Eu^{3+} aggregates, as shown from eight samples of the $Na_xEu^{3+}{}_{(2-x)/3}MoO_4$ series. Different amounts of Eu^{3+}-dimers have been detected in six modulated and ordered crystal structures, characterized by weak satellite reflections appearing in the lower angle part of their XRD pattern. The correlations between relative amounts of Eu^{3+} dimers on one hand, and the quantum yields, Q_L^{Eu} and Q_{Eu}^{Eu}, and lifetimes, τ_{obs}, on the other hand, are very close to linearity.

This study points to the importance of considering the superspace formalism without which no direct correlation could be found between composition and luminescent properties of the material. Once the superspace model is established, it is straightforward to explore all the configuration modes and deduce the structures with the largest number of Eu^{3+} dimers in order to maximize luminescence. With this in mind, we can claim that the superspace concept represents a predictive tool for the discovery of new physical properties in material sciences. It would be thus challenging to test the luminescent properties of some extended series of SRCs with general composition $M_{n/m}XO_4 = A^+{}_xB^{2+}{}_yC^{3+}{}_z(X^{6+}O_4)^{2-}$, where $n/m = x + y + z \leq 1$ and the valence condition, $x + 2y + 3z = 2$, defines the formula neutrality. The proposed compositions permit vacancies variation from 0 to 33%, many of them can have incommensurately modulated structure with different arrangement of $C^{3+} = Ln^{3+}$-dimers, which promote luminescence.

Acknowledgements

We thank the financial support of the Swiss National Science foundation, (grants No 20-105325/1, 200021-109470/1, and 200020_119866/1). V. Morozov is grateful for financial support of the Russian Foundation for Basic Research (Grant 08-03-00593). J.-C. G. Bünzli thanks the World Class University program (Photovoltaic Materials, Department of Materials Chemistry, Korea University) funded by the Ministry of Education, Science and Technology through the National Research Foundation of Korea (R31-10035).

Notes and references

1 R. J. Packer, S. J. Skinner, A. A. Yaremchenko, E. V. Tsipis, V. V. Kharton, M. V. Patrakeev and Y. A. Bakhteeva, *J. Mater. Chem.*, 2006, **16**, 3503.
2 X. Kuang, M. A. Green, H. Niu, P. Zajdel, C. Dickinson, J. B. Claridge, L. Jantsky and M. J. Rosseinsky, *Nat. Mater.*, 2008, **7**, 498.
3 B. Muktha, G. Madras and T. N. G. Row, *J. Photochem. Photobiol., A*, 2007, **187**, 177.
4 S. Neeraj, N. Kijima and A. K. Cheetham, *Chem. Phys. Lett.*, 2004, **387**, 2.
5 Z. L. Wang, H. B. Liang, L. Y. Zhou, H. Wu, M. L. Gong and Q. Su, *Chem. Phys. Lett.*, 2005, **412**, 313.
6 C. F. Guo, F. Gao, L. F. Liang, B. C. Choi and J. H. Jeong, *J. Alloys Compd.*, 2009, **479**, 607.
7 Z. L. Wang, H. B. Liang, M. L. Gong and Q. Su, *J. Alloys Compd.*, 2007, **432**, 308.
8 S. K. Shi, X. R. Liu, J. Gao and J. Zhou, *Spectrochim. Acta, Part A*, 2008, **69**, 396.
9 M. Thomas, P. P. Rao, M. Deepa, M. R. Chandran and P. Koshy, *J. Solid State Chem.*, 2009, **182**, 203.
10 L. Macalik, P. E. Tomaszewski, R. Lisiecki and J. Hanuza, *J. Solid State Chem.*, 2008, **181**, 2591.
11 A. P. A. Marques, M. T. S. Tanaka, E. Longo, E. R. Leite and L. L. V. Rosa, *J. Fluoresc.*, 2010, **21**, 893.
12 J. P. M. van Vliet, G. Blasse and L. H. Brixner, *J. Solid State Chem.*, 1988, **76**, 160.
13 T. Janssen, G. Chapuis and M. de Boissieu, *Aperiodic Crystals: from Modulated Phases to Quasicrystals*, Oxford University Press, Oxford, 2007.
14 A. Arakcheeva and G. Chapuis, *Acta Crystallogr., Sect. B: Struct. Sci.*, 2008, **64**, 12.
15 V. Petricek, M. Dusek and L. Palatinus, *Jana* 2006. Structure determination software Institute of Physics, Praha, Czech Republic, 2006.
16 A. Leineweber and V. Petricek, *J. Appl. Crystallogr.*, 2007, **40**, 1027.
17 J. Martinez-Garcia, A. Arakcheeva, P. Pattison, V. Morozov and G. Chapuis, *Philos. Mag. Lett.*, 2009, **89**, 257.
18 A. Aebischer, F. Gumy and J.-C. G. Bünzli, *Phys. Chem. Chem. Phys.*, 2009, **11**, 1346.
19 S. V. Eliseeva and J.-C. G. Bünzli, *Chem. Soc. Rev.*, 2010, **39**, 189.
20 D. Ananias, M. Kostova, F. A. A. Paz, A. N. C. Neto, R. T. De Moura, O. L. Malta, L. D. Carlos and J. Rocha, *J. Am. Chem. Soc.*, 2009, **131**, 8620.
21 Z. L. Wang, H. B. Liang, J. Wang, M. L. Gong and Q. Su, *Mater. Res. Bull.*, 2008, **43**, 907.
22 Z. L. Wang, H. B. Liang, M. L. Gong and Q. Su, *Opt. Mater.*, 2007, **29**, 896.
23 Z. L. Wang, H. Liang, M. L. Gong and Q. Su, *Mater.Lett.*, 2008, **62**, 619.
24 D. Xue, K. Betzler, H. Hesse and D. Lammers, *J. Phys. Chem. Solids*, 2002, **63**, 359.